

Application of Nano-Aluminum/Nitrocellulose Mesoparticles in Composite Solid Rocket Propellants

Gregory Young,^{*[a]} Haiyang Wang,^[b] and Michael R. Zachariah^[b]

Abstract: In this work we investigate the potential application of nano-aluminum/nitrocellulose mesoparticles as an ingredient for solid composite rocket propellants. The basic strategy is to incorporate nanoaluminum in the form of a micrometer scale particle containing a gas-generator, to enable easier processing, and potential benefits resulting from reduced sintering prior to combustion. The mesoparticles were made by electrospray and comprised aluminum nanoparticles (50 nm) and nitrocellulose to form micrometer scale particles. In this study, 80% solids loaded composite propellants (AP/HTPB based) were made with the addition of micrometer sized (2–3 μm) aluminum (10 wt-%), and

compared directly to propellants made by directly substituting aluminum mesoparticles for traditional micrometer sized particles. Propellant burning rate was relatively insensitive for mesoparticles containing between 5–15 wt-% nitrocellulose. However, direct comparison between a mesoparticle based propellant, to a propellant containing micrometer scale aluminum particles showed burning rates approximately 35% higher while having a nearly identical burning rate exponent. High speed imaging indicate that propellants using mesoparticles have less agglomeration of particles on the propellant surface.

Keywords: Mesoparticle · Nanoaluminum · Solid propellant · Electrospray

1 Introduction

Aluminum is a commonly used fuel supplement in solid rocket propellants because of its ability to increase the overall system level performance of a rocket motor. The addition of aluminum to composite rocket propellants increases the specific impulse as well as the density of the propellant, thereby increasing the total energy density. Aluminum also provides a secondary benefit of minimizing combustion instabilities by providing condensed phase particles, which can attenuate oscillatory behavior in a rocket motor. For these reasons aluminum combustion has been a topic of interest for a number of years.

Since typical aluminized composite propellant surface temperatures are about 800 K [1,2] and micrometer scale aluminum ignition generally occurs near 2000–2300 K [3–7], one should not expect that ignition of micrometer scale particles occurs in close proximity to the propellant surface. In fact, because the vaporization temperature of aluminum is at least 2700 K (pressure dependent), aluminum remains in the condensed phase sufficiently long such that fuel droplets can undergo aggregation and coalescence [8]. For these reasons, traditional micrometer scale aluminum has little impact on the burning rates of composite propellants. However, increases in propellant burning rate are desirable in order to improve the mass fraction of the propellant and ultimately system level performance of a solid rocket motor.

The replacement of micrometer-sized aluminum with nanoscale aluminum in the propellant matrix has shown to

increase propellant burning rates by as much as 100% [9,10]. In part, this can be attributed to the lower ignition temperatures [11,12] of aluminum nanoparticles in comparison to micrometer sized aluminum. Ignition of aluminum closer to the surface of the propellant increases the heat feedback to the propellant, which accelerates the decomposition process of the propellant matrix and ultimately the burning rate. However, due to the high specific surface area of nanoaluminum, significant problems with propellant processing are encountered [13–15]. The practical result is that it is difficult to make solid propellants using nanoaluminum with high solids loadings, thus minimizing many of its potential benefits as a propellant ingredient.

In this study we investigate the potential of employing nanoaluminum assembled into a micrometer scale particle. More specifically these aluminum mesoparticles [16] are formed through a rapid gelling of nanoaluminum with an

[a] G. Young
RDT&E Department
Naval Surface Warfare Center Indian Head Explosive Ordnance
Disposal Technology Division
Indian Head, MD 20640, USA
*e-mail: gregory.young1@navy.mil

[b] H. Wang, M. R. Zachariah
Department of Chemical and Biomolecular Engineering and
Department of Chemistry and Biochemistry
University of Maryland
College Park, MD 20742, USA

energetic binder (nitrocellulose) to create structure on the micrometer scale. Because the mesoparticles are on the same scale as typical aluminum powders they can be processed more easily than nanoparticles. On the other hand these micrometer scale particles still possess the same specific surface area of nanoaluminum. Thus they maintain many of the same combustion characteristics as nanoparticles, namely ignition temperature and ignition delay. Since the particles are held together by an energetic binder which serves as a gas generator, we further anticipate a minimization of particle agglomeration and or sintering. These materials were previously discussed by Wang et al. [16] indicating that ignition delay times of these aluminum mesoparticles were significantly reduced in comparison to the raw aluminum nanopowder used to form them. This would seem to indicate a further advantage of the mesoparticle concept over pure nanoaluminum. If the ignition process can be further enhanced by gelling with nitrocellulose, it would suggest that the aluminum particles in a propellant mixture would then ignite even closer to the propellant surface further increasing the heat feedback to the propellant and ultimately the burning rate.

2 Approach

2.1 Raw Materials and Sample Preparation

Aluminum/nitrocellulose mesoparticles were made by electrospray as a means to create a gel within a droplet by evaporation induced rapid aggregation of aluminum nanoparticles, containing a small mass fraction of an energetic binder. Details of this process can be found in Ref. [16]. The aluminum nanoparticles used to create the mesoparticles were originally purchased from the Argonide Corporation and designated as 50 nm ALEX by the supplier. Initially, particle morphology was studied by scanning electron microscope (SEM). As Figure 1 shows, the aluminum-nitrocellulose mesoparticles are typically between 2 μm and 16 μm . The size can be controlled by increasing the nano-Al particle concentration in the precursor solution.

Composite solid rocket propellants were formulated with mesoparticles containing nitrocellulose content ranging from 5 wt-% to 20 wt-% for comparison of combustion properties vs. traditional micrometer scale aluminum (Valimet H2). According to the supplier, H2 aluminum has a mean particle size between 2–3 μm per Fisher sub sieve. For each type of particle a propellant was formulated with 10 wt-% particle, 70 wt-% ammonium perchlorate (AP), and the balance hydroxyl-terminated polybutadiene (HTPB) binder for an 80% solids loaded propellant. We used a bimodal blend of AP with a coarse to fine ratio of 80/20 with coarse particles sieved to between 200 and 312 μm and fine particles sieved to between 45 and 90 μm . The AP was purchased from Kerr McGee and had a chemical purity of 99.8%. The HTPB binder was made up of a 50/50 blend of R45HT and Isodecyl Pelargonate (IDP), and was crosslinked

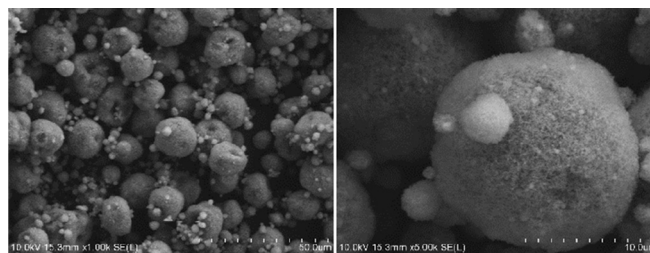


Figure 1. SEM images of 90 wt-% aluminum 10 wt-% nitrocellulose mesoparticles.

Table 1. Summary of propellant formulations.

Propellant designation	Nitrocellulose [wt-%]	Al [wt-%]	Aluminum type
1	0	10	Valimet H2
2	0.5	9.5	Mesoparticles with 5 wt-% NC
3	1	9	Mesoparticles with 10 wt-% NC
4	1.5	8.5	Mesoparticles with 15 wt-% NC
5	2	8	Mesoparticles with 20 wt-% NC

with Isophorone Diisocyanate (IPDI). Table 1 provides a summary of the propellant formulations and their designations. For our purposes propellant 1 was considered our baseline and the only difference between it and the others is the direct substitution of mesoparticles for the traditional micrometer scale aluminum.

The propellants were mixed by hand in 20 g batches and cast in a rectangular Teflon mold with a depth of approximately 0.635 cm (1/4"). The propellant samples were subjected to three vacuum cycles to remove any air that was entrapped during the mixing or casting processes. After curing at 60 °C for 48 h, the propellant samples were removed from the curing oven and square cross-section strands measuring 0.635 cm \times 0.635 cm \times 3.81 cm (1/4" \times 1/4" \times 1 1/2") were cut from the cast sample.

2.2 Experimental

Two main experiments were used to characterize the propellants in this study. First our propellant samples were subjected to simultaneous Thermal Gravimetric Analysis (TGA) and Differential Scanning Calorimetry (DSC) (TA Instruments SDT-Q600 Thermal Gravimetric Analyzer) to provide an understanding of their fundamental decomposition characteristics. All experiments were conducted in a nitrogen environment with a heating rate of 10 °C \cdot min⁻¹ in an alumina pan. Second, combustion studies were conducted using an optically accessible strand burner to determine the propellant burning rates with aluminum mesoparticles in comparison to micrometer scale aluminum as a function of pressure. Experiments were conducted with pressures up to about 4.25 MPa. Figure 2 provides a schematic diagram of the strand burning apparatus. The strand burner

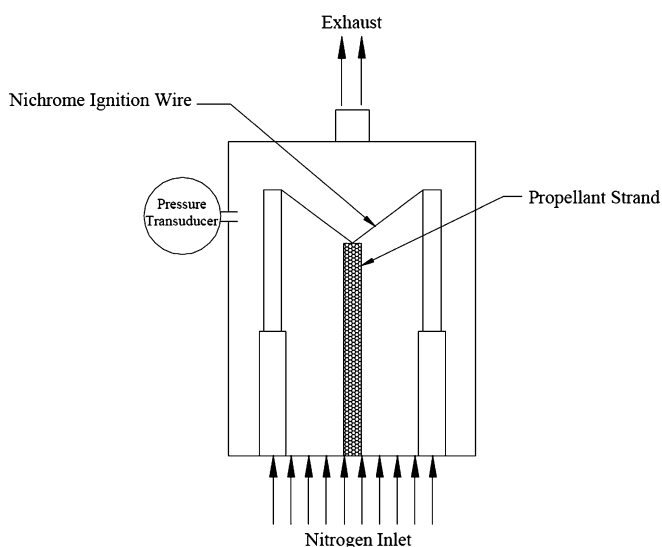


Figure 2. Schematic of strand burning apparatus.

used in this study had three optical ports allowing for viewing of the combusting sample. Propellant samples were ignited by resistive heating of a nichrome wire in a pressurized environment (nitrogen) and burning rate measurements were made by video record. During the experiment we ran a continuous purge of nitrogen to allow us to view the surface of the propellant and in turn to make the burning rate measurement. All samples were coated with nail polish prior to testing to limit the degree of side burning. Due to the limited number of samples available all experiments were conducted at room temperature conditions. Finally, we conducted several experiments in open air at 0.101 MPa (1 atm) to observe the burning surface of the propellant by high speed imaging. A Phantom V7.3 high speed camera was used to image the burning surface of propellants 1 and 4 to visualize any difference in combustion behavior. For these experiments all lighting, framing rates, and exposure times were held fixed.

3 Results and Discussion

3.1 Thermal Analysis

The results of the simultaneous TGA and DSC experiments can be seen in Figure 3 for propellants 1–4. Overall there is very little difference between the baseline propellant, and the propellants based on aluminum mesoparticles. According to the TGA results all of the samples appear to go through a three-step weight loss. At approximately 150 °C the first step begins and it ends at about 220 °C. A second weight loss occurs at about 300 °C, followed by the final weight loss which begins at about 350 °C. We attribute the initial weight loss to the decomposition of our plasticizer, IDP. The second weight loss occurring at about 300 °C also corresponds to an exothermic event. This event is likely the

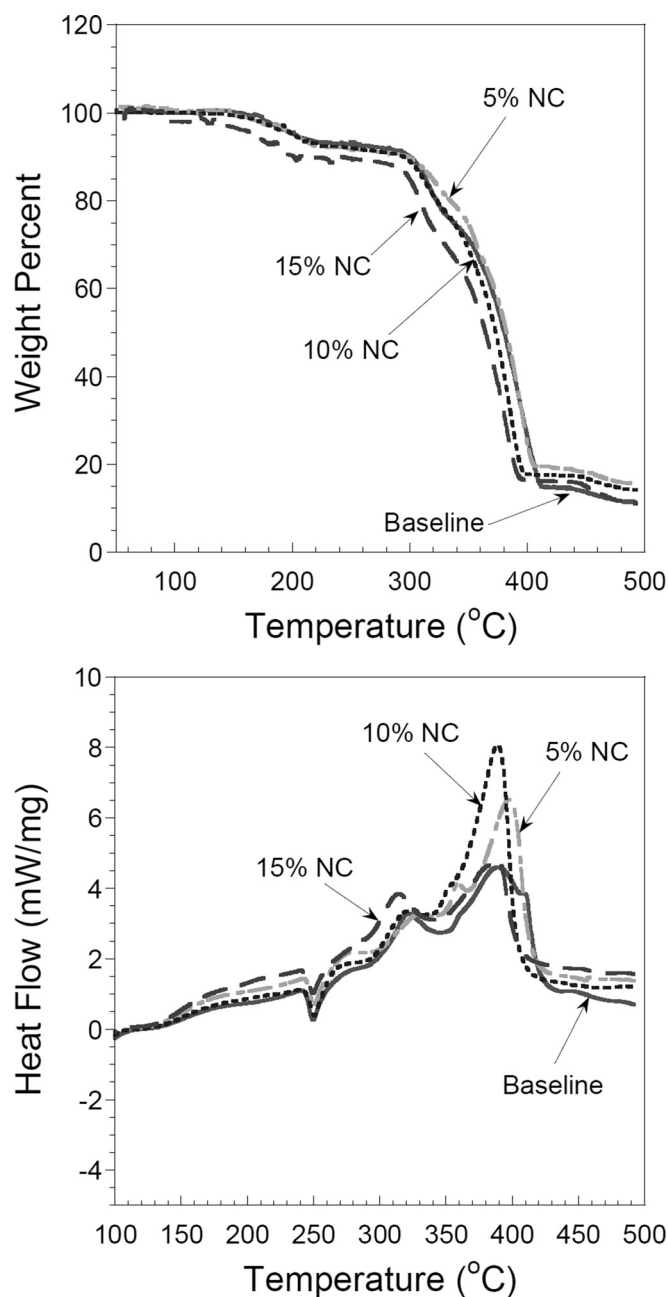


Figure 3. TGA (top) and DSC (bottom) of baseline and mesoparticle based propellants.

combination of two separate exothermic events. First AP is known to decompose exothermically in this temperature range [17–19], and second Lu and Kuo [20] demonstrated the exothermic decomposition of cured R45 with an isocyanate curing agent. The exothermic decomposition of cured HTPB in this temperature range is thought to be the result of the cleavage of the urethane linkage and depolymerization of the cured HTPB [20–22]. The endothermic event occurring at approximately 250 °C is consistent with the known AP phase transformation from orthorhombic to cubic [17,18]. The final weight loss near 350 °C is accompa-



Figure 4. Captured video images of baseline (top) and mesoparticle (bottom) propellant burning in strand burner at 4.25 MPa. Note luminosity increase in mesoparticle based propellant.

nied by the onset of another exothermic event. The weight loss starting at 350 °C is consistent with the decomposition of cured HTPB [20]. The exothermic nature of this event is a result of the interaction of the decomposing HTPB with the decomposition products of the decomposing AP.

3.2 Strand Burning Experiments

Figure 4 provides an example of the burning of both our baseline propellant, and a propellant with mesoparticle additives. For both sets of images the same lighting and camera settings were applied. In each case one-dimensional burning was established allowing for direct measurement of the burning rate. It is clear from the images in Figure 4 that the mesoparticle based propellant demonstrates a greater degree of luminosity particularly with respect to the propellant surface. This is an indication of aluminum particle ignition in close proximity to the propellant surface.

Initially a study was conducted, in which we systematically varied the nitrocellulose content of the mesoparticles from 5 wt-% to 20 wt-% to determine the burning rate sen-

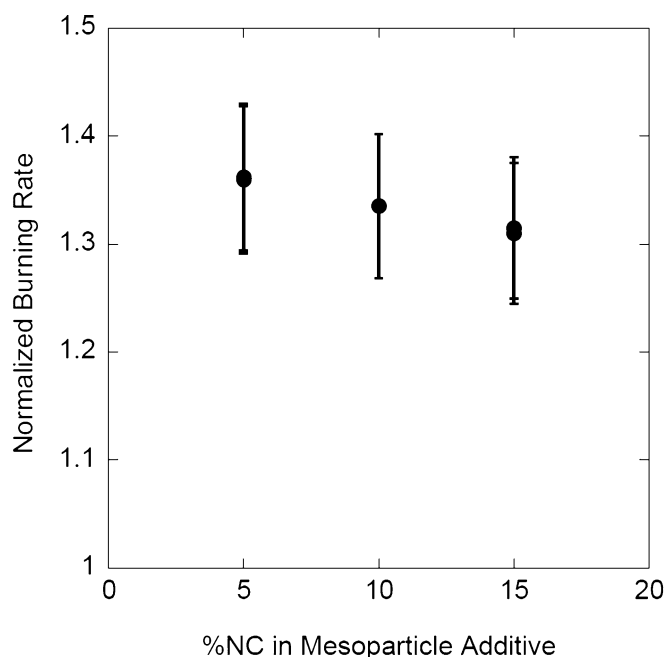


Figure 5. Propellant burning rate as a function of mesoparticle nitrocellulose content.

sitivity to that variable. All of these experiments were conducted at approximately 4.25 MPa. In each case three experiments were conducted in order to provide an indication of repeatability. The results shown in Figure 5 are the burning rates normalized by propellant 1. Propellants with mesoparticles containing 20 wt-% nitrocellulose (propellant 5) blew apart during testing, and therefore these results are not included. Figure 5 shows a clear linear burning rate enhancement by direct replacement of traditional micrometer scale aluminum with aluminum/nitrocellulose mesoparticles to be as large as 35% and slightly decreasing with nitrocellulose content. Aluminum does not generally affect propellant burning rates significantly for traditional micrometer scale aluminum, however in this study we used Valimet H2 aluminum in our baseline which may contribute positively to burning rate since it is less than 10 μm [15]. This may be one reason our burning rate benefit, and those observed with nanoaluminum by other researchers differ [9,10]. Since the burning rates of the mesoparticle propellants were not significantly different, all subsequent experiments were conducted with mesoparticles containing 15 wt-% nitrocellulose.

We next examined the effects of pressure, for our mesoparticle based propellant (propellant 4) in comparison to our baseline propellant (propellant 1), which was varied from about 0.9 MPa to 4.25 MPa. As can be seen in Figure 6 both propellants were found to follow the traditional St. Robert's Burning Rate Law with nearly identical pressure exponents, 0.49 for propellant 1 and 0.50 for propellant 4. For practical purposes in a full rocket motor, these pressure

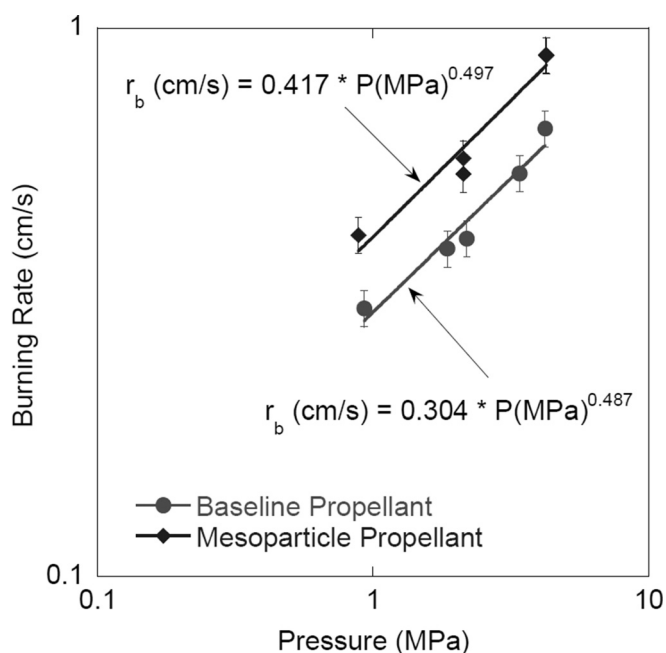


Figure 6. Comparison of burning rates between Propellant 1 and Propellant 4 as a function of pressure.

exponents are reasonably low, and would be perfectly suitable for safe and reliable rocket motor application.

3.3 Imaging of the Burning Surface

A series of experiments were conducted allowing the propellant to burn in air at 0.101 MPa (1 atm) to view the burning surface by high speed imaging. By comparing Figure 7

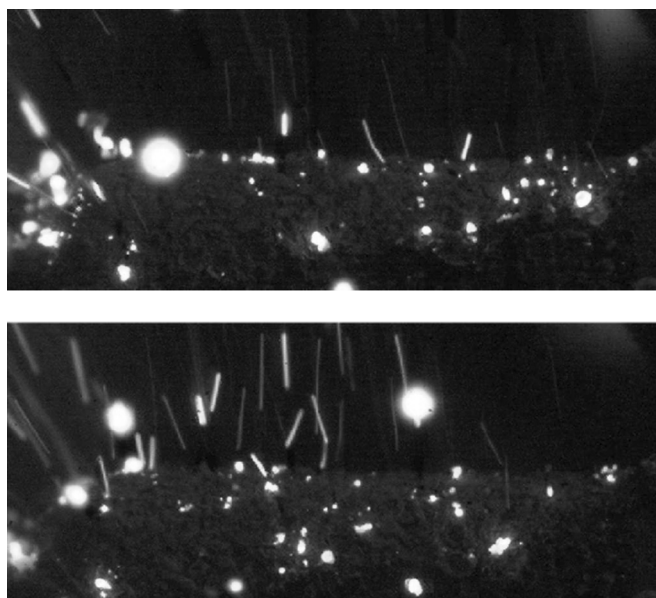


Figure 7. High speed images of Propellant 1 (baseline) burning at atmospheric pressure.

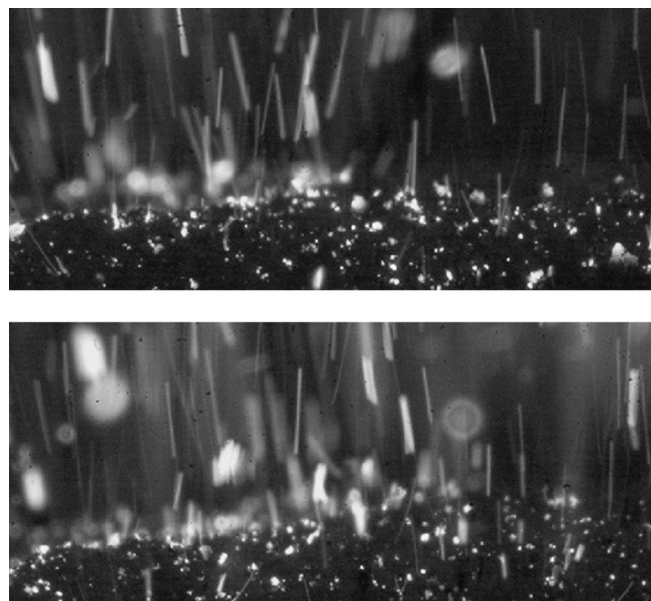


Figure 8. High speed images of Propellant 4 (mesoparticle based) burning at atmospheric pressure.

and Figure 8 some clear differences of the near propellant surface combustion between the micrometer aluminum based propellant (Propellant 1) and mesoparticle based propellant (Propellant 4) can be seen. By mass the same amount of aluminum particle was in each propellant, and the particle sizes when considering the assembled mesoparticle were similar. Qualitatively it is quite clear that the ignited particle density at or very near the propellant surface is far greater for the mesoparticle based Propellant 4. Furthermore the particles which have clearly reached ignition in Propellant 1, are significantly larger than the particles observed in Propellant 4 suggesting that they were far more susceptible to agglomeration at the surface. This result is consistent with our prior work on the implementation of mesoparticles that showed that assembly of nanoparticles with a low-temperature gas generator leads to a decreased sintering, and enhanced burning [16,23–25]. The decrease in agglomeration provides an additional practical benefit of the mesoparticles since it would imply a reduction in two phase flow loss in a rocket motor.

4 Conclusion

An experimental study was conducted to study the potential application of aluminum/nitrocellulose mesoparticles as a fuel for solid rocket propellants. These mesoparticles are comprised of a gelled nanoaluminum with varying amounts of nitrocellulose, to form a micrometer scale particle comprised of nanoscale components. 80% solids loaded composite propellants were formulated based on ammonium perchlorate (70%) and aluminum (10%) with the balance

being HTPB binder. Propellants were formulated with mesoparticles containing between 5–20 wt-% nitrocellulose as well as traditional micrometer sized aluminum. When compared directly to those of a propellant using traditional micrometer scale aluminum (2–3 μm), the mesoparticle based propellant had burning rates approximately 35% higher with nearly identical burning rate exponents ca. 0.5. High speed imaging of the propellants burning at atmospheric pressure revealed that the mesoparticle based propellants seem to undergo less surface agglomeration. The results of this study suggest that mesoparticles could be an attractive alternative to nanoparticles for propellant formulations by significantly outperforming propellants using micrometer sized aluminum of a similar size while offering the potential of processing benefits which plague nanoparticles.

Acknowledgments

The authors would like to acknowledge the support of the Defense Threat Reduction Agency through grant number HDTRA1-14-1-0038 as well as Dr. Mitat Birkan from the Air Force Office of Scientific Research.

References

- [1] C. Zanotti, A. Volpi, M. Boanichessi, L. De Luca, *Measuring Thermodynamic Properties of Burning Propellants*, in: *Nonsteady Burning and Combustion Stability of Solid Propellants*, Vol. 143, *Progress in Astronautics and Aeronautics* (Eds.: L. De Luca, E. W. Price, M. Summerfield), AIAA, Reston, VA, **1992**, p. 145.
- [2] E. W. Price, R. K. Sigman, *Combustion of Aluminized Solid Propellants*, in: *Solid Propellant Chemistry, Combustion, and Motor Interior Ballistics*, Vol. 185, *Progress in Astronautics and Aeronautics* (Eds.: K. K. Kuo, M. Summerfield), AIAA, Reston, VA, **2000** p. 663.
- [3] V. A. Ermakov, A. A. Razdobreev, A. I. Skorik, V. V. Pozdeev, S. S. Smolyakov, Temperature of Aluminum Particles at the Time of Ignition and Combustion, *Combust Explos. Shock Waves* **1982**, *18*, 256–257.
- [4] R. Friedman, A. Macek, Ignition and Combustion of Aluminum Particles in Hot Ambient Gases, *Combust. Flame* **1962**, *6*, 9–19.
- [5] R. Friedman, A. Macek, Combustion Studies of Single Aluminum Particles, *Proc. Combust. Inst.* **1963**, *9*, 703–709.
- [6] T. A. Brzustowski, I. Glassman, *Spectroscopic Investigation of Metal Combustion*, in: *Heterogeneous Combustion*, Vol. 15, *Progress in Astronautics and Aeronautics* (Eds.: H. G. Wolfhard, I. Glassman, L. Green Jr.), AIAA, Reston, VA, **1964** p. 41.
- [7] D. K. Kuehl, Ignition and Combustion of Aluminum and Beryllium, *AIAA J.* **1965**, *3*, 2239–2247.
- [8] E. W. Price, *Combustion of Metallized Propellants*, in: *Fundamentals of Solid Propellant Combustion*, Vol. 90, *Progress in Astronautics and Aeronautics* (Eds.: K. K. Kuo, M. Summerfield), AIAA, Reston, VA, **1984** p. 479.
- [9] L. T. DeLuca, L. Galfetti, G. Colombo, F. Maggi, A. Bandera, Microstructure Effects in Aluminized Solid Rocket Propellants, *J. Propul. Power* **2010**, *26*, 724–733.
- [10] L. Galfetti, L. T. DeLuca, F. Severini, L. Meda, G. Marra, M. Marchetti, M. Regi, S. Belluci, Nanoparticles for Solid Rocket Propulsion, *J. Phys. Condens. Matter* **2006**, *18*, S1991–S2005.
- [11] T. Bazyn, H. Krier, N. Glumac, Combustion of Nanoaluminum at Elevated Pressure and Temperature Behind Reflected Shock Waves, *Combust. Flame* **2006**, *145*, 703–713.
- [12] R. A. Yetter, G. A. Risha, S. F. Son, Metal Particle Combustion and Nanotechnology, *Proc. Combust. Inst.* **2009**, *32*, 1819–1838.
- [13] L. Galfetti, L. DeLuca, F. Severini, G. Colombo, L. Meda, G. Marra, Pre and Post-Burning Analysis of Nano-Aluminized Solid Rocket Propellants, *Aero. Sci. Technol.* **2007**, *11*, 26–32.
- [14] Z. Jiang, S.-F. Li, F.-Q. Zhao, Z.-R. Liu, C.-M. Yin, Y. Luo, S.-W. Li, Research on the Combustion Properties of Propellants with Low Content of Nano Metal Powders, *Propellants Explos. Pyrotech.* **2006**, *31*, 139–147.
- [15] A. Dokhan, E. W. Price, J. M. Seitzman, R. K. Sigman, The Effect of Bimodal Aluminum with Ultrafine Aluminum on the Burning Rates of Solid Propellants, *Proc. Combust. Inst.* **2002**, *29*, 2939–2945.
- [16] H. Wang, J. Guoqiang, S. Yan, J. B. DeLisio, C. Huang, M. R. Zachariah, Electro Spray Formation of Gelled Nano-Aluminum Microspheres with Superior Reactivity, *Appl. Mater. Inter.* **2013**, *5*, 6797–6801.
- [17] D. Majda, A. Korobov, U. Filek, B. Sulikowski, P. Midgley, D. Vowles, J. Klinowski, Low-Temperature Thermal Decomposition of Large Single Crystals of Ammonium Perchlorate, *Chem. Phys. Lett.* **2008**, *454*, 233–236.
- [18] V. V. Boldyrev, Thermal Decomposition of Ammonium Perchlorate, *Thermochim. Acta* **2006**, *443*, 1–36.
- [19] G. Young, C. Roberts, S. Dunham, Combustion Behavior of Solid Oxidizer/Gaseous Fuel Diffusion Flames, *J. Propul. Power* **2013**, *29*, 362–370.
- [20] Y. C. Lu, K. K. Kuo, Thermal Decomposition Study of Hydroxyl-Terminated Polybutadiene (HTPB) Solid Fuel, *Thermochim. Acta* **1996**, *275*, 181–191.
- [21] J. K. Chen, T. B. Brill, Chemistry and Kinetics of Hydroxyl-Terminated Polybutadiene (HTPB) and Diisocyanate-HTPB Polymers During Slow Decomposition and Combustion-Like Conditions, *Combust. Flame* **1991**, *87*, 217–232.
- [22] C. W. Fong, B. L. Hamshere, The Mechanism of Burning Rate Catalysis in Composite HTPB AP Propellant Combustion, *Combust. Flame* **1986**, *65*, 61–69.
- [23] H. Wang, G. Jian, J. DeLisio, M. R. Zachariah, “Microsphere Composites of Nano-Al and Nanothermites: An Approach to Better Utilization of Nanomaterials, 52nd Aerospace Sciences Conference, National Harbor, MD, USA, January 13–16, **2014**, AIAA-0647.
- [24] P. Chakrabort, M. R. Zachariah, Do Nano-Energetic Particles Remain Nano-Sized During Combustion, *Combust. Flame* **2014**, *161*, 1408–1416.
- [25] H. Wang, G. Jian, J. Delisio, M. R. Zachariah, Assembly and Reactive Properties Al/CuO Nanothermite Microparticles, *Combust. Flame* **2014**, *161*, 2203–2220.

Received: January 28, 2015

Revised: February 23, 2015

Published online: April 16, 2015